INFORMATION MODEL FOR SELECTING THE OPTIMAL SPATIAL FORM OF PARTS

ANTON PANDA[1], KOSTIANTYN DYADYURA[2], SVETLANA ANTOSHCHUK[3], IGOR PROKOPOVICH[4]

[1]Faculty of Manufacturing Technologies with a seat in Presov, Technical University of Kosice, Bayerova 1, 080 01 Presov, Slovak Republic

[2]Department of Biomedical Engineering, Odesa Polytechnic National University, Shevchenka Ave 1, 65044 Odesa, Ukraine, dyadyura.k.o@op.edu.ua

[3]Odesa National Polytechnic University, Shevchenka Ave 1, Odesa, 65044, Ukraine, asg@op.edu.ua

[4]Department Of Design Information Technologies and Design, Odesa Polytechnic National University, Shevchenka Ave 1, 65044 Odesa, Ukraine, igor.prokopovich@gmail.com

DOI: 10.17973/MMSJ.2024_11_2024026

e-mail: anton.panda@tuke.sk

A complex of interrelated methods and means of analysis, clustering, segmentation and classification of objects on images obtained by sensors of different physical nature (with the help of modern methods of radiography, computer and magnetic resonance imaging) is proposed, which will allow modeling the optimal form of a bone substitute with functional properties by CAD/CAM/CAE design methods, depending on the anatomical data, the nature and localization of the cavity bone defect, its size, load conditions and patterns of bone tissue neoplasm.

Methods for making multi-criteria decisions have been developed, which will allow for their implementation for a wide range of optimization tasks of researching the correlation of the shape and size of porosity with indicators of the stress-deformed state of bone substitutes in order to maintain the structural integrity of the biomaterial in the process of regeneration of hard tissue.

KEYWORDS

machine learning, decision making, tissue engineering, computed tomographic, bone image segmentation, artificial intelligence, craniotomy, craniectomy skull implants, thickness measurements, automated design, training data sets

1 INTRODUCTION

Craniocerebral trauma is damage to the bones of the skull and soft tissues - blood vessels, brain, nerves, meninges, etc. In medical practice, it is considered one of the most difficult and unpredictable injuries, because the consequences of damage can manifest themselves after several years - in the form of violations of vital functions, disorders of the nervous system, and disability.

In modern military conflicts, injuries of a neurosurgical profile are distributed as follows: Damage to the soft tissues of the head — 50%, penetrating wounds of the skull — 28%, non-penetrating injuries — 17% [Laskowitz 2023]. The specific weight of mine-explosive damage, which reaches 70% of combat injuries, is increasing [Heath 2023, Brichacek 2021]. Combined damage is noted in about 30%, multiple — in 7% of the victims [Aita 2023]. In the ongoing war in Ukraine, the frequency of head trauma is 37.5%, of which gunshot and explosive injuries are 7.9%, and closed cranial brain injury is 12.7% [Shchehlov 2024]. Cranioplasty refers to the operation of filling and restoring a defective skull with different repair materials [Alkhaibary 2020]. It is currently one of the most routine neurosurgical operations and can be performed in many primary care hospitals. The anatomical curvature of the skull (Fig. 1.) and its facial bone is extremely complex, and for skilled surgeons, it is often necessary to precisely align and restore the implant.

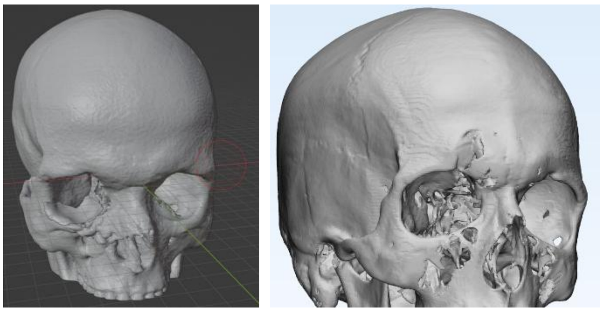

a) b)

Figure 1. 3D imaging of the patient's skull: (a) coronal plane of the preoperative computed tomography (b) volume imaging technique revealed the defect

Cranial implants must have an appropriate convex shape and precisely fit the defect border. The main criterion for a successful assessment of the cranial area is an anatomically plausible, symmetrical shape with a smooth and seamless fit along the defect border [Worm 2019]. The results of research given in the works [Zaborowski 2007, Adamcik 2014, Svetlik 2014, Rimar 2016, Olejarova 2017, Sedlackova 2017, Catlos 2018, Labun 2018, Gamec 2019, Murcinkova 2019, Pollak 2019 & 2020, Straka 2021 & 2022, Vagaska 2021, Czyzewski 2022, Csamer 2023] show that cranioplasty not only restores the shape of the skull cavity, but also achieves the effect of restoration of aesthetics, and also plays an important role in the restoration of the patient's neurological function. The use of 3D printing technology in the field of cranioplasty, which involves the reconstruction of skull defects, has become an advanced possibility of anatomical shape change [Morais 2019]. Although autologous bone or preformed titanium meshes can be used as implants, 3D-printed implants have proven to be more versatile and have a number of other advantages, such as personalization and improved biocompatibility, lower risk of complications or lower likelihood of needing secondary surgery [Chen 2017]. Automatic acquisition of fast and accurate estimates of implant shapes can lead to increased efficiency in the clinical cranioplasty workflow. Modeling of the shape of cranial implants is performed in computer aided design (CAD) software based on the processing of patient diagnostic imaging data, allowing for the precise design and manufacture of custom implants (PSIs) that match the patient's unique anatomy. Numerical modeling using Finite Element Analysis (FEA) is used to optimize the design of individual implants taking into account mechanical loading. The European Union (EU) Medical Device Regulations (MDR 2017/745, Clause 30) allows the use of open-source solutions. Designing cranial implants usually requires a lot of human computer interaction (3D modeling skills) and medical expertise (sufficient knowledge of cranial anatomy) [Monkova 2013, Michalik 2014, Panda 2014 & 2021, Baron 2016, Mrkvica 2016, Balara 2018, Chaus 2018, Duplakova 2018, Sukhodub 2018, Flegner 2019 & 2020, Harnicarova 2019, Pandova 2020, Wu 2022], especially in cases of defects reaching both sides of the skull [Fishman 2024].

Traditional methods of skull reconstruction use the mirror image of the healthy side of the skull on the defective side [Kim 2021], surface interpolation [Iaccarino 2020], or a combination of them [Kodym 2021, Pisaneschi 2024] to estimate the skull area. At the same time, given the fact that skull defects can cross the plane of symmetry, and the bones of the human skull are usually asymmetric, it is impractical to use a mirror image operation to create the geometry of the implant. In recent years, methods of skull shape reconstruction based on volumetric convolutional neural networks have shown great promise in this regard [Yin 2024]. A widely used approach now is the U-Net and its variants [Yao 2024]. Segmentation of medical images is a critical task in the use of deep learning [Saeed 2022]. The selection of regions of interest (ROIs) is a common step in medical image analysis for all imaging modalities. Various methods were used to perform the task of segmentation. There is a problem with incomplete data when performing segmentation of volumetric medical images (3D segmentation) [Chen 2019]. This problem is not computationally solvable. Therefore, optimization methods are used to calculate the solution [Zhang 2023].

Recently, synthetic datasets for automatic evaluation of skull regions have become available because they are easy to generate from public databases of healthy skulls, such as CQ500 [Ostas 2022]. However, they do not necessarily fully capture the distribution of skull shape defects in the target clinical data (ie, different anatomical variability of the target population, shapes and sizes of defects, complex morphology of the defect border), which may affect the quality of reconstruction in practice. On the other hand, it is difficult to obtain real clinical data with implant models designed by experts. Furthermore, in our experience, the distribution of available clinical data is often skewed toward simple unilateral defect cases and is difficult to extend with synthetic defects and implant shapes. More complex bilateral and fronto-orbital defects are less common, but it is in these complex cases that correct autocranial reconstruction or implant design can have the greatest impact on clinical practice. Therefore, it is desirable to develop a method that can use data from both types of cranioplasty.

The main goal of this article is to discuss the use of some aspects of non-equilibrium phase transitions for the development of an information model for choosing the optimal spatial shape of a bone substitute using the example of cranial implants. The use of this approach takes into account geometric and physical modeling nonlinearities.

2 MATERIALS AND METHODS

Let us assume that the system can receive a certain set of data described by the state vector q. We describe the image by an N are dimensional vector q (Fig. 1), the individual components of which are features encoded using numbers. Let us also assume that the detection system consists of elements j and that element j measures the q_j (feature) component of the vector q.

Trajectories consisting of several consecutive time steps of dynamics define a path between elements i and j with the probability of choosing a certain path, for example, $i \to j$, given that the trajectory starts from element i, therefore, is determined by the product of the corresponding transition probabilities. The transition probabilities, p_{ij}, are conditional by definition, assuming that the initial state of the transition is i. Consequently, the unconditional probability $i \to j$ can be expressed (Bayes formula) $q_{ij} = x_i \cdot p_{ij}$, where x_i is the probability of choosing element i.

If there is a stationary process, then the incoming signals satisfy the probability distribution $f(q)$. We will assume that some images are presented to the system again and again and that these images correspond to the maxima of the probability distribution

$$f(q) = max \quad (1)$$

Suppose the system can measure moments

$$\langle q_i \rangle, \langle q_i q_j \rangle, \langle q_i q_j q_k \rangle, \langle q_i q_j q_k q_l \rangle \quad (2)$$

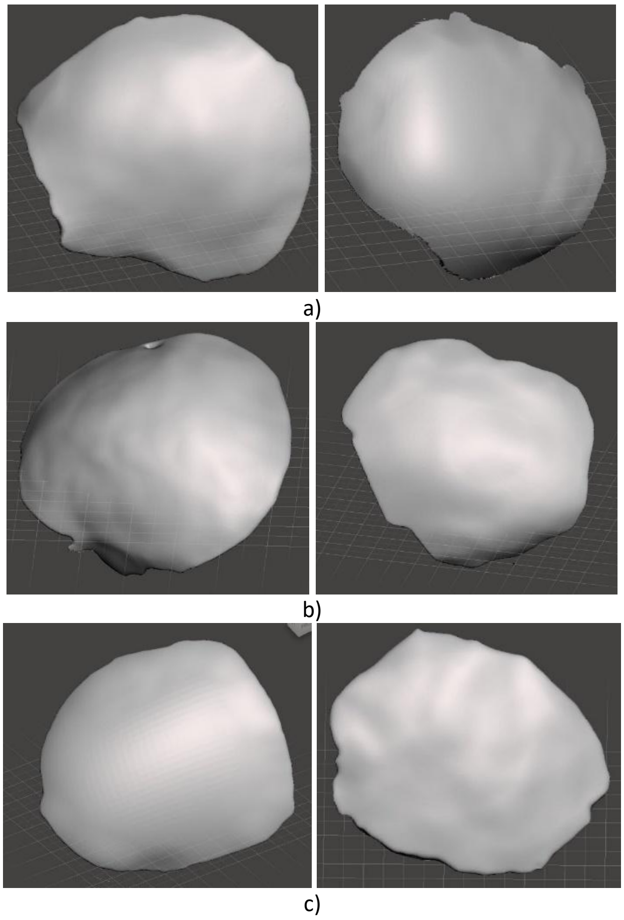

Figure 2. Detailed input and output datasets: a) the upper parts of the defective skulls are displayed in the top view and the isometric view (generation of patches, c determination of the area of contact with the support base); b) complete skulls generated by the proposed system; c) ideal (main) implants and created implants

To reconstruct the function $f(q)$ from these moments, we will use the principle of maximum information entropy and try to understand what minimum order of moments is necessary to obtain a reasonable function f. If we limit ourselves to linear moments only, then, according to the principle of maximum information entropy, the function f should have the following form: $f(q) = N \cdot exp(-\lambda \cdot q)$, where λ is a real number.

The function f(q) cannot be normalized in the space of vectors q if the variables q takes values from minus to plus infinity, so it is impossible to limit ourselves to only linear moments. If we use moments up to the second order inclusive, then the general form of the distribution function will be as follows [Valicek 2016]

$$f(q) = N \cdot exp(\bar{\alpha} \cdot q + \bar{q} \cdot \alpha - \bar{q} \cdot B \cdot q) \quad (3)$$

By introducing a new variable ξ using the relation

$$q = \xi + B^{-1} \cdot \alpha \quad (4)$$

We can write function (3)

$$\tilde{f}(\xi) = N' \cdot exp(-\bar{\xi} \cdot B \cdot \xi) \quad (5)$$

Since B is a positive definite matrix, the maximum of function (5) can be achieved only at one value of the variable ξ, namely at $\xi = 0$.

By making the change of variables (4), we realize that in our model there is only one maximum, i.e. only one image is kept. In reality, a set of images is usually presented for recognition. This contradiction leads us to the need to consider moments up to and including the fourth order. For simplicity, we will assume that odd-order moments are equal to zero. In this case, in accordance with the principle of maximum information entropy, the distribution function has the following form:

$$f(q) = N \cdot exp\big(-\sum_{i,j} \lambda_{i,j} \cdot q_i \cdot q_j - \sum_{i,j,m,n} \lambda_{i,j,m,n} \cdot q_i \cdot q_j \cdot q_m \cdot q_n\big) \tag{6}$$

Now we will show how you can construct a network that implements function (6). Let us assume that the distribution function (6) arises as a result of a continuous stationary Markov process described by the Fokker-Planck equation [Jurko 2011], where in our case V is the still unknown potential.

$$f = \sum_k \frac{\partial}{\partial q_k}\left(\frac{\partial V}{\partial q_k} \cdot f\right) + \frac{Q}{2} \cdot \sum_k \frac{\partial^2 f}{\partial q_k^2} \tag{7}$$

To establish the connection between the distribution function (6) and the still unknown quantities V and Q in equation (7), for brevity, we denote the parentheses on the right side of relation (6)

$$\big(-\sum_{i,j} \lambda_{i,j} \cdot q_i \cdot q_j - \sum_{i,j,m,n} \lambda_{i,j,m,n} \cdot q_i \cdot q_j \cdot q_m \cdot q_n\big) = -\tilde{V}(q,\lambda) \tag{8}$$

We will require that the stochastic forces F_j in the Langevin equation [Jurko 2012] corresponding to equation (7) satisfy the relations

$$\begin{gathered} \langle F(t) \rangle = 0, \\ \langle F_i(t) \cdot F_j(t') \rangle = Q \cdot \delta_{ij} \cdot \delta \cdot (t - t') \end{gathered} \tag{9}$$

Moreover, let

$$\tilde{V} = \frac{2 \cdot V}{Q} \tag{10}$$

The Langevin equation corresponding to the Fokker-Planck equation (7) is of the form [Jurko 2013]

$$q'_j = -\frac{\partial V}{\partial q_j} + F_j(t) \tag{11}$$

The potential V is determined by relationships (8), (10), i.e. measurement results. We're getting

$$-\frac{\partial V}{\partial q_i} = Q \cdot \left\{\sum_j \lambda_{ij} \cdot q_i + 2 \cdot \sum_{j,m,n,} \lambda_{i,j,m,n} \cdot q_i \cdot q_j \cdot q_m \cdot q_n\right\} \tag{12}$$

Equation (11), in which the first term on the right-hand side is determined by relation (12), takes a particularly simple form for the network. Thus, it is possible to build a network that implements the distribution function $f(q)$, if the second and fourth moments of this function are known. The purpose of the network is only to transfer the value of the quantity q_j, multiplied by the "synaptic strength" λ_{ij}, from element i to element j (the first term on the right side of relation (12)) or transmit the value $q_j q_m q_n$, multiplied by λ_{ijmn} from elements j, m, n to element i (the second term on the right side of relation (12)), then in the corresponding element i summation is carried out (Fig.3).

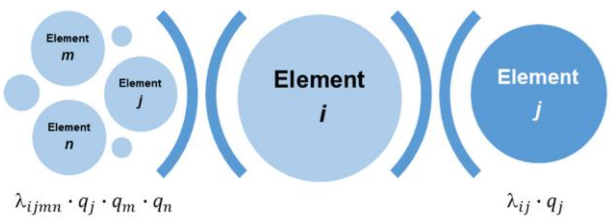

Figure 3. Network purpose

One more completely general and important conclusion is true. If the network can measure only a very specific set of correlation functions (1) (or higher order ones), then it is only necessary to include the corresponding terms in expression (12). The existence of attractor states in potential dynamics leads to the fact that any initial state turns out to be attracted to one of the local minima of the potential $V(q)$, which are located at points corresponding to the prototypes of the images. If the initial state is sufficiently close to one of these minima, then this minimum is realized and the initially incomplete image is supplemented, i.e., the entire mechanism acts as a kind of associative memory and hence has the ability to recognize patterns.

Let us determine the values of the coefficients λ_{ij} and λ_{ijmn}. Let $f(q)$ be the given distribution function of images entering the system, and $\tilde{f}(q)$ be the distribution function generated by the system. Let us introduce as a measure of the distance between these two functions the increase in information (Kullback information) [Panda 2011]

$$K = \int f(q) \cdot ln\left(\frac{f(q)}{\tilde{f}(q)}\right) \cdot d^N \cdot q \geq 0, \tag{13}$$

Where we need to consider two restrictions

$$\begin{gathered} \int f(q) \cdot d^N \cdot q = 1, \\ \int \tilde{f}(q) \cdot d^N \cdot q = 1 \end{gathered} \tag{14}$$

Since the function $f(q)$ is specified, and expression (13) can be represented in the form

$$K = \int f(q) \cdot lnf(q) \cdot d^N \cdot q - \int \tilde{f}(q) \cdot lnf(q) \cdot d^N \cdot q \tag{15}$$

It is sufficient to find the maximum of the expression

$$\int f(q) \cdot ln\tilde{f}(q) \cdot d^N \cdot q = max \tag{16}$$

To determine this, let us assume that the function f has the form

$$\tilde{f} = exp\left[-\tilde{\lambda} - \sum_j \tilde{\lambda}_j \cdot V_j(q)\right] \tag{17}$$

Where the potential V_j can contain polynomials with respect to q, the degree of which does not exceed some limit specified by us; $\tilde{\lambda}_j$ – parameters that can be varied [Panda 2013]. The left side of expression (16) (multiplied by -1) can be represented as

$$W \equiv -\int f(q) \cdot ln\tilde{f}(q) \cdot d^N \cdot q = \tilde{\lambda} + \int f(q) \cdot \sum_j \tilde{\lambda}_j \cdot V_j(q) \cdot d^N \cdot q \tag{18}$$

We assume that $\tilde{\lambda}_j$ are subject to an evolutionary strategy, for example, fluctuations in connectivity may occur in the network. The most elegant evolutionary strategy is one that uses gradients of some potential. Let us choose the function W given by relation (18) as the potential to be minimized and assume that

$$\tilde{\lambda} = ln \int exp\left[-\sum_j \tilde{\lambda}_j \cdot V_j(q)\right] \cdot d^N \cdot q \tag{19}$$

The gradient strategy comes down to representing the Lagrange multipliers $\tilde{\lambda}_j$ in the form [Zaloga 2019]

$$\tilde{\lambda}'_j = -\gamma \cdot \frac{\partial W}{\partial \tilde{\lambda}_j} \tag{20}$$

To calculate the right-hand side of this equality, we substitute expression (19) into formula (18) and form a derivative

$$\frac{\partial W}{\partial \lambda_j} = -\left[\left\{\int exp\left\{-\sum_j \tilde{\lambda}_j \cdot V_j(q) \cdot d^N\right\}^{-1} \cdot \int V_j(q) \cdot exp\left\{-\sum_j \tilde{\lambda}_j \cdot V_j(q) \cdot d^N\right\}\right\} \cdot d^N\right] + \int f(q) \cdot V_j(q) \cdot d^N \cdot q \tag{21}$$

As simple arguments show, the expression on the right side of relation (21), enclosed in rectangular brackets, can be interpreted as the average value

$$\left[\left\{\int exp\{-\textstyle\sum_j \tilde{\lambda}_j \cdot V_j(q) \cdot d^N\}^{-1} \cdot \int V_j(q) \cdot exp\{-\textstyle\sum_j \tilde{\lambda}_j \cdot V_j(q) \cdot d^N\}\right\} \cdot d^N\right] = \langle V_j \cdot (q)\rangle_{\tilde{f}} \qquad (22)$$

While the last term on the right side of relation (21) is the mean value $\langle V_j \cdot (q)\rangle_f$.
Therefore, equation (20) can be written very briefly as

$$\tilde{\lambda}'_j = \gamma \cdot \left(\langle V_j \cdot (q)\rangle_{\tilde{f}} - \langle V_j \cdot (q)\rangle_f\right) \qquad (22)$$

Where the first term on the right side is the average of V_j according to the distribution function $\tilde{f}$, the second term is the average of the same potential V_j, but according to the distribution function specified by external conditions. By comparing these two values, the decision-making system (neural network) can appropriately adjust the connections $\tilde{\lambda}$ between its elements and thus learn to perform its task.
The software implementation of the proposed methods of learning neural networks based on nonlinear dynamics was developed and their approbation was carried out when building a segmentation and classification subsystem. Neural network training methods were further developed based on the proposed modifications of the gradient descent method, which made it possible to reduce the training time of neural networks of various architectures when solving the tasks of object segmentation and classification. To solve the problem of segmentation, the architecture of a hybrid convolutional neural network based on a pre-trained ResNet-18 network coder and a decoder from the U-Net network was chosen. As an error function, it is proposed to use a linear combination of cross-entropy and the Dice coefficient [Zaloga 2020], which has proven itself well in training convolutional neural networks. Training was conducted using the PyTorch library with various modifications of the gradient descent method.

3 RESULTS

The simulation process is presented in the form of the following scheme (Fig. 4). The proposed research methodology adopted for the reconstructive project consisted of five steps, as shown in Figure 4. The cranioplasty procedure begins with the integration of a defective 3D model of the skull using a dataset of image data, CT scans, which are converted into digital image and communication files in Medicine (DICOM). When performing CT of the desired anatomy, it is recommended that the spatial resolution of the images does not exceed 1.25 mm. The dataset used for this study is DICOM (digital image) metadata. The DICOM data is then further processed by medical image processing software to create a 3D model of the scanned defective skull bone. To reduce the computational load, the study reduced the resolution of the 3D model and generated only the upper part of the skull with a volume resolution of 112 × 112 × 40. Second stage: data preparation, including segmentation of the desired anatomy from the acquired DICOM data and generation of CAD 3D models, reconstruction and registration using the developed technique. The open source 3D Slicer software environment was used for visualization, segmentation, registration and analysis of medical, biomedical and other 3D images, as well as for planning and navigation of the images. The curvature of the implant was reconstructed with 12 automatically generated patches. The third stage: development of a predictive model, which includes two phases: training and prediction. Fourth stage: three-dimensional shape prediction based on the predictive model developed and optimized in the second stage. The standard tessellation language (STL) file of the model is imported into the slicing software, where an a.gcode file is created containing predefined parameters such as the 3D printing material used and the layer height. At the fifth stage, the final form of the cranial implant required for surgical intervention was produced using additive technology.

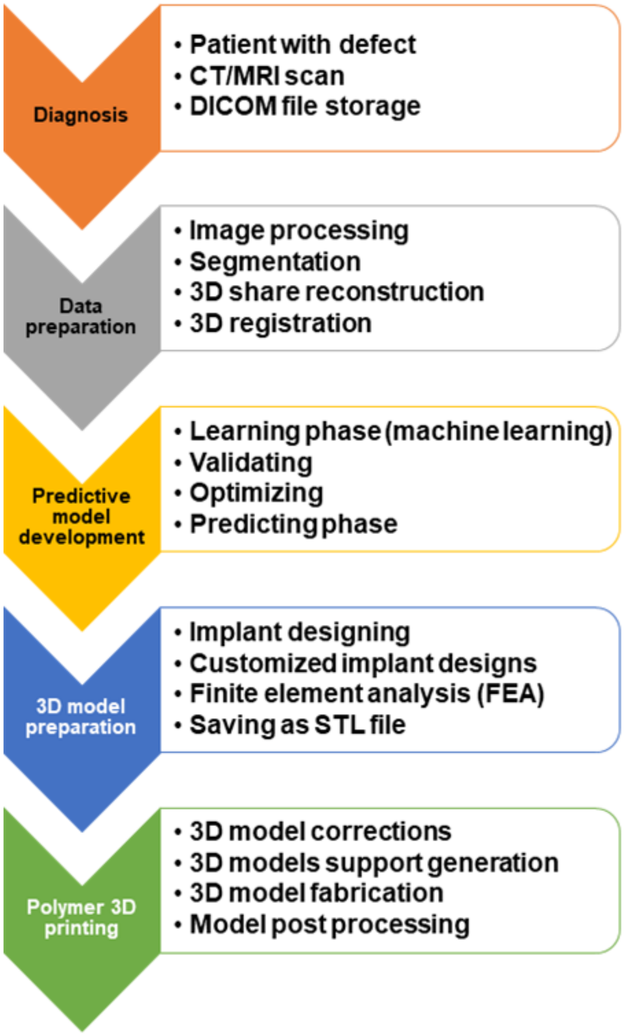

Figure 4. A block diagram illustrating the stages of selecting a technique for implant reconstruction

A Markforged x7 printer was used to fabricate composite material samples with variable stiffness and strength through thickness. The designs of the obtained samples were tested for increased resistance to damage. Materials consisting of continuous carbon fibers, as well as an onyx matrix reinforced with chopped carbon fibers were used for the production of samples by additive technology. Continuous carbon fibers have the following parameters: a diameter of 1.75 mm, a bending stiffness of 57 GPa, a bending strength of 540 MPa. Onyx matrix fibers are a short nylon thermoplastic reinforced with carbon fibers. This design and structure ensures the rigidity, durability and precision of the parts, and is more than 1.4 times stronger than ABS. Characteristics of onyx: diameter 1.75 mm, bending stiffness 2.9 GPa, strength 81 MPa. The skull plate was printed in the orientation shown in Fig. 5. The implant has a constant thickness, different from the original bone, and a certain spatial tolerance along the border of the defect to allow for scar tissue and continued bone growth, allowing for implantation.
There were no significant typographical errors or discrepancies. This resulted in an acceptable 3D model, structured according to the CT data and ready for implantation. The main criterion for a successful assessment of a cranial patch is an anatomically plausible, symmetrical shape with a smooth and seamless fit along the defect border (Fig. 6). After 3D printing, plates are

sterilized in a low-temperature sterilizer with hydrogen peroxide plasma. Implants are prepared during surgery Anatomical models printed on 3D printing were used for subsequent craniotomy surgery.

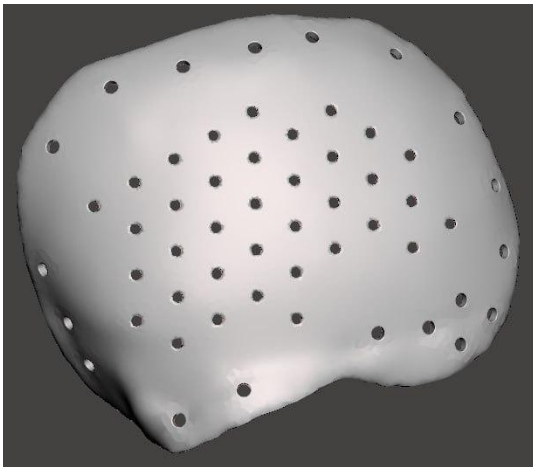

Figure 5. 3D model fabrication

To analyze the morphology of the surface, observations were made using scanning electron microscopy (TS5130-Tescan SEM at 20 kV accelerated voltage) (Fig. 7).

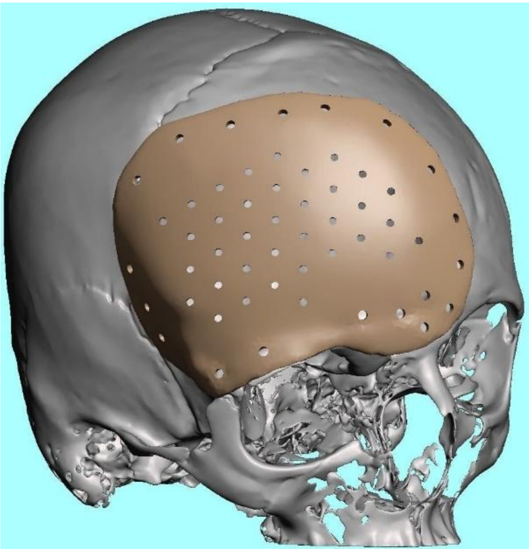

Figure 6. Graphical comparison Finding the best reconstruction technique

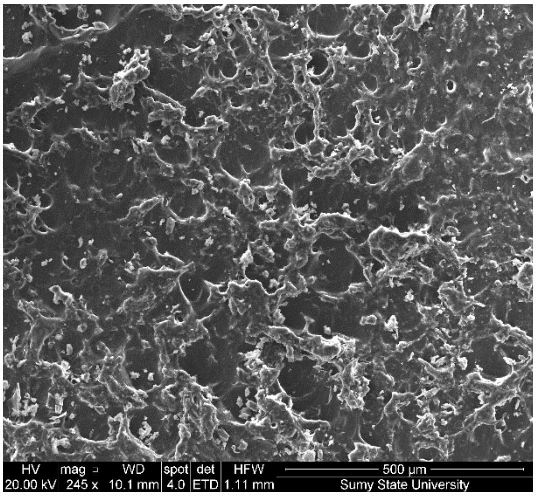

Figure 7. Scanning electron microscopy images of samples

One can observe the fibrous surface. On the surface, there are equiaxed depressions along with microcavities. The morphology of the surface is consistent with the mechanical characteristics of the material, which were given earlier [Gulyaev 2022].

4 CONCLUSIONS

The human skull is one of the most complex parts of the body. The creation of individualized endoprostheses by cranioplasty is necessary in the case of a post-traumatic or postoperative defect to ensure a decent quality of life for the victims. Despite certain disadvantages, the use of 3D-printed implants remains the best possible option in everyday use in terms of time savings, anatomical accuracy and appropriate cosmetic effects.

Traditionally, the implant is designed semi-automatically using CAD software. The input of such a semi-automatic design process is a defective skull, and the output is an implant. There is an urgent need for automatic design of cranial implants. The motivation for such work is the need to automate this process and improve the quality of medical care.

Deep learning networks, used to predict a full skull or an additional part, can be trained on a dataset. The paper proposed an algorithm for segmentation of the region of interest on the image based on the application of nonequilibrium phase transitions, which provides new ideas and analogies between different approaches to the segmentation process. In this article, a fourth-order chaotic system is proposed, accompanied by the analysis of the Lagrange exponent and bifurcations.

The proposed system is designed to detect diagnostically significant study areas for automated image analysis using neural network training methods based on nonlinear dynamics. Future work may focus on increasing the number of skull models combined with appropriate data enhancement technology and network architecture mechanisms, which will improve the learning quality of the decision-making system and increase the volumetric resolution. It is also possible to carry out further research on the recognition of skull defects of different sizes based on the positions of non-equilibrium phase transitions.

ACKNOWLEDGMENTS

This work was supported by the project VEGA 1/0226/21 of Scientific Grant Agency of the Ministry of Education, Science, Research and Sport of the Slovak Republic and the Slovak Academy of Sciences.

REFERENCES

[Adamcik 2014] Adamcik, F., et al. Modeling of Changes in Flow Air Fuel Effected by Changes in Environmental Conditions. Nase More, 2014, Vol. 61, No.1-2., pp. 40-42. ISSN 0469-6255.

[Aita 2023] Aita, S.L., et al. Posttraumatic Stress Disorder Complicated by Traumatic Brain Injury: A Narrative Review. SN Compr. Clin. Med., 2023, Vol. 5, 92.

[Alkhaibary 2020] Alkhaibary, A., et al. Cranioplasty: A comprehensive review of the history, materials, surgical aspects, and complications. World Neurosurg., 2020, Vol. 139, pp. 445-452.

[Balara 2018] Balara, M., Duplakova, D., Matiskova, D. Application of a signal averaging device in robotics. Measurement, 2018, Vol. 115, No. 2, pp. 125-132.

[Baron 2016] Baron, P., Dobransky, J., Kocisko, M., Pollak, M., Cmorej, T. The parameter correlation of acoustic emission and high-frequency vibrations in the assessment process of the operating state of the technical system. Acta Mechanica et Automatica, 2016, Vol. 10, No. 2, pp. 112-116.

[Brichacek 2021] Brichacek, M., et al. Decision-making in adult cranial vault reconstruction. Plast Reconstr Surg, 2021, Vol. 148, pp. 109E-121E.

[Catlos 2018] Catlos, M., et al. Continual Monitoring of Precision of Aerial Transport Objects. In: 13th International Scientific Conference on New Trends in Aviation Development (NTAD); Kosice, 30-31 August, 2018. New York: IEEE, pp 30-34. ISBN 978-1-5386-7918-0.

[Chaus 2018] Chaus, A.S., Pokorny, P., Caplovic, E., Sitkevich, M.V., Peterka, J. Complex fine-scale diffusion coating formed at low temperature on high-speed steel substrate. Applied Surface Science, 2018, Vol. 437, pp. 257-270. ISSN 0169-4332.

[Chen 2017] Chen, X., Xu, L., Li, X., Egger, J. Computer-aided implant design for the restoration of cranial defects. Sci. Rep., 2017, Vol. 23, 4199.

[Chen 2019] Chen, X., et al. Learning active contour models for medical image segmentation. In: Proceedings of the IEEE Conference on Computer Vision and Pattern Recognition, 2019, 11632-11640. DOI: 10.1109/CVPR.2019.01190.

[Csamer 2023] Csamer, L., et al. Custom-made 3D printing-based cranioplasty using a silicone mould and PMMA. Sci Rep, 2023, Vol. 13, 11985.

[Czyzewski 2022] Czyzewski, W., et al. Low-cost cranioplasty-a systematic review of 3D printing in medicine. Materials, 2022, Vol. 15, 4731.

[Dmytriiev 2024] Dmytriiev, D., Garland, E.L. Chronic pain during 60 days of war: the impact of the Russian war on Ukrainian patients. J Public Health, 2024. DOI: 10.1007/s10389-024-02243-w.

[Duplakova 2018] Duplakova, D., et al. Determination of optimal production process using scheduling and simulation software. Int. J. of Simulation Modelling, 2018, Vol. 17, No. 4, p. 447.

[Fishman 2024] Fishman, Z., et al. Thickness and design features of clinical cranial implants—what should automated methods strive to replicate? Int J CARS, 2024, Vol. 19, pp. 747-756.

[Flegner 2019] Flegner, P., Kacur, J., Durdan, M., Laciak, M. Processing a measured vibroacoustic signal for rock type recognition in rotary drilling technology. Measurement, 2019, Vol. 134, pp. 451-467.

[Flegner 2020] Flegner, P., Kacur, J., Durdan, M, Laciak, M. Statistical Process Control Charts Applied to Rock Disintegration Quality Improvement. Applied Sciences, 2020, Vol. 10, No. 23, pp. 1-26.

[Gamec 2019] Gamec, J., et al. Low Profile Sinuous Slot Antenna for UWB Sensor Networks. Electronics, 2019, Vol. 8, No. 2, pp 1-11. ISSN 2079-9292.

[Gulyaev 2022] Gulyaev, P., et al. Particle and Particle Agglomerate Size Monitoring by Scanning Probe Microscope. Applied Sciences, 2022, Vol. 12, No. 4. DOI: 10.3390/app12042183.

[Harnicarova 2019] Harnicarova, M., et al. Study of the influence of the structural grain size on the mechanical properties of technical materials. Materialwissenschaft und Werkstofftechnik, 2019, Vol. 50, No. 5, pp. 635-645.

[Heath 2023] Heath, K.M., et al. Blast-Related Traumatic Brain Injury and Concomitant Post-Traumatic Stress Disorder: a Review of Overlapping Symptoms. Curr Phys Med Rehabil Rep, 2023, Vol. 11, pp. 377-383.

[Iaccarino 2020] Iaccarino, C., et al. Cranioplasty following decompressive craniectomy. Front Neurol, 2020, Vol. 10, 1357.

[Jurko 2011] Jurko, J., Gajdos, M., Panda, A. Study of changes under the machined surface and accompanying phenomena in the cutting zone during drilling of stainless steels with low carbon content. Metalurgija, 2011, Vol. 50, No. 2, pp. 113-117.

[Kim 2021] Kim, M.J., Lee, H.B., Ha, S.K., Lim, D.J., Kim, S.D. Predictive factors of surgical site infection following cranioplasty: A study including 3D printed implants. Front Neurol, 2021, Vol. 12, 745575.

[Kodym 2021] Kodym, O., Spanel, M., Herout, A. Deep learning for cranioplasty in clinical practice: Going from synthetic to real patient data. Comput Biol Med, 2021, Vol. 137, 104766.

[Labun 2018] Labun, J., et al. Possibilities of Increasing the Low Altitude Measurement Precision of Airborne Radio Altimeters. Electronics, 2018, Vol. 7, No. 9, pp. 1-9. ISSN 2079-9292.

[Laskowitz 2023] Laskowitz, D.T., Van Wyck, D.W. ApoE Mimetic Peptides as Therapy for Traumatic Brain Injury. Neurotherapeutics, 2023, Vol. 20, pp. 1496-1507.

[Liu 2019] Liu, J., et al. A novel fourth order chaotic system and its algorithm for medical image encryption. Multidim Syst Sign Process, 2019, Vol. 30, pp. 1637-1657.

[Macala 2017] Macala, J., Pandova, I., Panda, A. Zeolite as a prospective material for the purification of automobile exhaust gases. Mineral Resources Management, 2017, Vol. 33, No. 1, pp. 125-137.

[Michalik 2014] Michalik, P., Zajac, J., Hatala, M., Mital, D., Fecova, V. Monitoring surface roughness of thin-walled components from steel C45 machining down and up milling. Measurement, 2014, Vol. 58, pp. 416-428. ISSN 0263-2241.

[Monkova 2013] Monkova, K., Monka, P., Jakubeczyova, D. The research of the high speed steels produced by powder and casting metallurgy from the view of tool cutting life. Applied Mechanics and Materials, 2013, Vol. 302, pp. 269-274.

[Morais 2019] Morais, A., Egger, J., Alves, V. Automated computer-aided design of cranial implants using a deep volumetric convolutional denoising autoencoder. In: World Conference on Information Systems and Technologies, 2019, pp. 151-160. DOI: 10.1007/978-3-030-16187-3_15.

[Mrkvica 2016] Mrkvica, I., Neslusan, M., Cep, R., Sleha, V. Properties and comparison of PVD coatings. Technical Gazette, 2016, Vol. 23, No. 2, pp. 569-574.

[Murcinkova 2019] Murcinkova, Z., Vojtko, I., Halapi, M., Sebestova, M. Damping properties of fibre composite and conventional materials measured by free damped vibration response. Advances in Mechanical Engineering, Vol. 11, No. 5, 1687814019847009.

[Olejarova 2017] Olejarova, S., Dobransky, J., Svetlik, J., Pituk, M. Measurements and evaluation of measurements of vibrations in steel milling process. Measurement, 2017, Vol. 106, pp. 18-25.

[Ostas 2022] Ostas, D., et al. Point-of-care virtual surgical planning and 3D printing in oral and cranio-maxillofacial surgery: A narrative review. J Clin Med, 2022, Vol. 11, 6625.

[Panda 2014] Panda, A., Prislupcak, M., Pandova, I. Progressive technology diagnostics and factors affecting machinability. Applied Mechanics and Materials, 2014, Vol. 616, pp. 183-190.

[Panda 2021] Panda, A., Anisimov, V.M., Anisimov, V.V., Dyadyura, K., Pandova, I. Increasing of wear resistance of linear block-polyurethanes by thermal processing methods. MM Science Journal, 2021, Vol. October, pp. 4731-4735.

[Pandova 2018] Pandova, I., et al. Use of sorption of copper cations by clinoptilolite for wastewater treatment. Int. J. of Environmental Research and Public Health, 2018, Vol. 15, No. 7, 1364.

[Pandova 2020] Pandova, I., et al. A study of using natural sorbent to reduce iron cations from aqueous solutions. Int. J. of Environmental Research and Public Health, 2020, Vol. 17, No. 10, 3686.

[Pisaneschi 2024] Pisaneschi, G., et al. Numerical and experimental investigation of a 3D-printed PCU patient-specific cranial implant. Prog Addit Manuf, 2024, Vol. 9, pp. 299-313.

[Pollak 2019] Pollak, M., Kascak, J., Teliskova, M., Tkac, J. Design of the 3D printhead with extruder for the implementation of 3D printing from plastic and recycling by industrial robot. TEM Journal, 2019, Vol. 8, No. 3, pp. 709-713.

[Pollak 2020] Pollak, M., Torokova, M., Kocisko, M. Utilization of generative design tools in designing components necessary for 3D printing done by a robot. TEM Journal, 2020, Vol. 9, No. 3, pp. 868-872.

[Rimar 2016] Rimar, M., Smeringai, P., Fedak M., Kuna S. Technical and software equipment for the real time positioning control system in mechatronic systems with pneumatic artificial muscles. Key Engineering Materials, 2016, Vol. 669, pp. 361-369.

[Saeed 2022] Saeed, S., et al. Hybrid grabcut hidden markov model for segmentation. Computers, Materials & Continua, 2022, Vol. 72, No. 1, pp. 851-869.

[Sedlackova 2017] Sedlackova, N.A, et al. Synthesis Criterion of Ergatic Base Complex with Focus on its Reliability. In: 14th IEEE Int. Sci. Conf. on Informatics; Poprad, 14-19 November, 2017. New York: IEEE, pp. 318-321. ISBN 978-1-5386-0889-0.

[Shchehlov 2024] Shchehlov, D., et al. First Experience of Treatment of Multiple Shrapnel Traumatic Pseudoaneurysms During the War in Ukraine Using Tegus Telemedical System. Clin Neuroradiol, 2024, Vol. 34, pp. 263-267.

[Straka 2021] Straka, L., Pitel, J., Corny, I. Influence of the main technological parameters and material properties of the workpiece on the geometrical accuracy of the machined surface at WEDM. Inter. J. of Advanced Manuf. Technology, 2021, Vol. 115, No. 9-10, pp. 3065-3087.

[Straka 2022] Straka, L., Gombar, M., Vagaska, A., Kuchta, P. Efficiency Optimization of the Electroerosive Process in μ-WEDM of Steel MS1 Sintered Using DMLS Technology. Micromachines, 2022, Vol. 13, 1446.

[Sukhodub 2018] Sukhodub, L., Panda, A., Dyadyura, K., Pandova, I., Krenicky, T. The design criteria for biodegradable magnesium alloy implants. MM Science J., 2018, Vol. December, pp. 2673-2679.

[Sukhodub 2019] Sukhodub, L., et al. Hydroxyapatite and zinc oxide based two-layer coating, deposited on Ti6Al4V substrate. MM Science J., 2019, Vol. December, pp. 3494-3499.

[Svetlik 2014] Svetlik, J., Baron, P., Dobransky, J., Kocisko, M. Implementation of Computer System for Support of Technological Preparation of Production for Technologies of Surface Processing. Applied Mechanics and Materials, 2014, Vol. 613, p. 418. DOI: 10.4028/www.scientific.net/AMM.613.418.

[Vagaska 2021] Vagaska, A., Gombar, M. Mathematical Optimization and Application of Nonlinear Programming. Studies in Fuzziness and Soft Computing, 2021, Vol. 404, pp. 461-486. DOI: 10.1007/978-3-030-61334-1_24.

[Valicek 2016] Valicek, J., et al. Mechanism of Creating the Topography of an Abrasive Water Jet Cut Surface. Advanced Structured Materials, 2016, Vol. 61, pp. 111-120.

[Wang 2022] Wang, J.Z., et al. Clinical applications of machine learning in predicting 3D shapes of the human body: a systematic review. BMC Bioinformatics, 2022, Vol. 23, 431.

[Worm 2019] Worm, P.V., Finger, G., do Nascimento, T.L., Rynkowski, C.B., Collares, M.V. The impact of cranioplasty on the patients' quality of life. J Craniomaxillofac Surg, 2019, Vol. 47, pp. 715-719.

[Wu 2022] Wu, CT., Yang, YH. & Chang, YZ. Three-dimensional deep learning to automatically generate cranial implant geometry. Sci Rep, 2022, Vol. 12, 2683.

[Yao 2024] Yao, W., Bai, J., Liao, W. et al. From CNN to Transformer: A Review of Medical Image Segmentation Models. J Digit Imaging. Inform. med. 2024, Vol. 37, No. 4, pp. 1529-1547.

[Yin 2024] Yin, Aa., Zhang, X., He, Yl. et al. Machine learning prediction models for in-hospital postoperative functional outcome after moderate-to-severe traumatic brain injury. Eur J Trauma Emerg Surg. 2024, Vol. 50, No. 4, pp. 1219-1228.

[Zaborowski 2007] Zaborowski, T. Ekowytwarzanie. Gorzow, 2007, 100 p.

[Zaloga 2019] Zaloga, V., Dyadyura, K., Rybalka, I., Pandova, I. Implementation of Integrated Management System in Order to Enhance Equipment Efficiency. Management Systems in Production Engineering, 2019, Vol. 4, pp. 221-226.

[Zaloga 2020] Zaloga, V., Dyadyura, K., Rybalka, I., Pandova, I., Zaborowski, T. Enhancing efficiency by implementation ofintegrated management system in order to align organizational culture and daily practice. Management Systems in Production Engineering, 2020, Vol. 28, No. 4, pp. 304-311.

[Zhang 2023] Zhang, S., Han, C. & Wang, W. Optimal Control and Stabilization for Discrete-time Markov Jump Systems With Indefinite Weight Costs and Multi-channel Multiplicative Noises. Int. J. Control Autom. Syst., 2023, Vol. 21, pp. 2162-2174.

CONTACTS:

Anton Panda, Prof. Eng., PhD.
Faculty of Manufacturing Technologies with a seat in Presov
Technical University of Kosice
Sturova 31, 080 001 Presov, Slovakia
anton.panda@tuke.sk